

# SYNCHRONISATION OF BIOLOGICAL CLOCK SIGNALS

## *Capturing Coupled Repressilators from a Control Systems Perspective*

Thomas Hinze, Mathias Schumann and Stefan Schuster

Department of Bioinformatics, Friedrich Schiller University Jena, E.-Abbe-Platz 1-4, D-07743 Jena, Germany

**Keywords:** Chronobiology, Coupled repressilators, Reaction-diffusion kinetics, Internal/external clock synchronisation, Control system, Phase-locked loop.

**Abstract:** Exploration of chronobiological systems emerges as a growing research field within bioinformatics focusing on various applications in medicine, agriculture, and material sciences. From a systems biological perspective, the question arises whether biological control systems for regulation of oscillative signals and their technical counterparts utilise similar mechanisms. If so, modelling approaches and parameterisation adopted from building blocks can help to identify general components for clock synchronisation. Phase-locked loops could be an interesting candidate in this context. Both, biology and engineering, can benefit from a unified view. In a first experimental study, we analyse a model of coupled repressilators. We demonstrate its ability to synchronise clock signals in a monofrequent manner. Several oscillators initially deviate in phase difference and frequency with respect to explicit reaction and diffusion rates. Accordingly, the duration of the synchronisation process depends on dedicated reaction and diffusion parameters whose settings still lack to be sufficiently captured by comprehensive tools like the Kuramoto approach.

## 1 INTRODUCTION

In both spheres, biological and technical systems, oscillatory signals play a major role in order to trigger and control time-dependent processes. Core oscillators are the simplest devices for generation of continuously running clock signals. To this end, signal processing units consisting of at least one feedback loop can suffice (Russo and di Bernardo, 2009). So, it is no surprise that probably numerous evolutionary origins led to oscillative reaction networks while independently technical attempts succeeded in construction of single clocks or clock generators.

The situation becomes more complicated if several of those core oscillators start to interact. Resulting biological systems are commonly driven to achieve a synchronous behaviour towards an evolutionary advantage. Correspondingly, clock synchronisation in technical systems is frequently inspired by the need to follow a global time. Interestingly, the formalisation of clock synchronisation processes is quite distant from each other. While in distributed computer systems, stepwise algorithmic approaches (like Berkeley or Cristian's method, (Tanenbaum and van Steen, 2001)) predominate, biological systems adjust their clock signals more gradually. Its

formalisation is either based on reaction-diffusion kinetics or employs the more abstract Kuramoto method (Kuramoto, 1984), an analytic signal coherence measure restricted to sinusoidal signal shape to counteract phase shift between each pair of core oscillators.

We define different temporally oscillating signals to be *synchronous* to each other if and only if they meet three conditions: (1) The oscillatory signal must run *undamped* to avoid signal weakening. (2) *Asymptotical or total harmonisation* of the oscillatory signals meaning that after a finite amount of time called  $t_{\text{sync}}$  (time to synchronisation), both temporal signal courses converge within an arbitrarily small  $\epsilon$ -neighbourhood. (3) The resulting oscillatory signal after  $t_{\text{sync}}$  has to be *monofrequent* to ensure chronoscopy (constant progression of time measure).

The central prerequisite of a core oscillator to be capable of synchronisation to others is its ability to vary its oscillation frequency within a specified range (Granada and Herzog, 2009). This variation can be achieved by *forcing*, by *resetting*, or by specific *selective perturbations* affecting the oscillating signal. Without any external influences, core oscillators resume their individual free-running oscillatory behaviour, mostly by losing their synchronicity.

Topologically, clock synchronisation can be ac-

accomplished by two different strategies called *external* and *internal* (Pikovsky et al., 2001). External strategies comprise a central leading clock that propagates its time signal throughout the whole network of downstream core oscillators which adjust their individual signals by accelerating or slowing down their frequency for a certain amount of time. Here, we observe an unidirectional coupling from the leading central clock to all others. In contrast, internal strategies aim at a mutual clock exchange between the network members. The coupling topology is mostly bidirectional, and each involved core oscillator is going to adjust its signal based on a weighted sum of the signals released by its adjacent clocks.

Within a case study, we exemplify internal synchronisation by a biological system composed of bidirectionally coupled repressilators. To this end, we model the entire gene regulatory networks using reaction-diffusion kinetics. Afterwards, we conduct two comprehensive simulation studies. The first one discloses the time to synchronisation subject to initial phase shift between the elementary repressilators. Its balanced diffusion rate acts as coupling strength. It appears that synchronisation of initially antiphase signals is most time-consuming for weak coupling while it has a negligible effect for strong coupling. A second simulation study investigates the synchronisation behaviour with respect to different initial frequencies of the single repressilators. The obtained numerical results are envisioned to identify building blocks and their parameterisation towards composition of a control system following the concept of phase-locked loops.

## 2 INTERNAL SYNCHRONISATION: COUPLED REPRESSILATORS

### 2.1 Reaction Network and Kinetics

We identified a network of bidirectionally coupled repressilators to be an appropriate candidate to explore internal synchronisation within a biological system. A repressilator is a gene regulatory network consisting of three focal proteins (LacI, TetR, cI) that mutually inhibit their expression from genes (*lacI*, *tetR*, *cI*) (Elowitz and Leibler, 2000). We employ a system composed of two coupled repressilators located in two adjacent cells inspired by Garcia-Ojalvo (Garcia-Ojalvo et al., 2004), see Fig. 1.

Let TetR be a protein able to migrate between the cells, it acts as coupling element. Its diffusion rate *diff* specifies the variable bidirectional coupling strength.

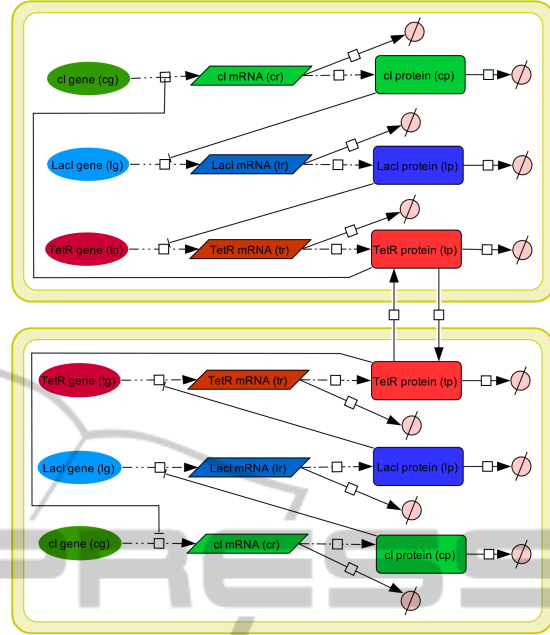


Figure 1: Network topology of the TetR-coupled repressilator model with diffusion between both core oscillators.

The dynamical behaviour of the network can be specified by reaction-diffusion kinetics based on corresponding ordinary differential equations (ODEs). For species names in the ODEs, we abbreviate (LacI, TetR, cI) = (*lp*, *tp*, *cp*) for the proteins and (*lacI*, *tetR*, *cI*) = (*lr*, *tr*, *cr*) for the mRNA. The set of equations for each single repressilator reads:

$$\begin{aligned}
 \frac{d lp}{d t} &= k_{lr} \cdot lr - k_{lp} \cdot lp \\
 \frac{d tp}{d t} &= k_{tr} \cdot tr - k_{tp} \cdot tp - diff \cdot tp + diff \cdot tp_{\text{external}} \\
 \frac{d cp}{d t} &= k_{cr} \cdot cr - k_{cp} \cdot cp \\
 \frac{d lr}{d t} &= \alpha_0 + \frac{\alpha \cdot k_m^n}{k_m^n + cp} - k_{lr} \cdot lr - k_{lr2} \cdot lr \\
 \frac{d tr}{d t} &= \alpha_0 + \frac{\alpha \cdot k_m^n}{k_m^n + lp} - k_{tr} \cdot tr - k_{tr2} \cdot tr \\
 \frac{d cr}{d t} &= \alpha_0 + \frac{\alpha \cdot k_m^n}{k_m^n + tp} - k_{cr} \cdot cr - k_{cr2} \cdot cr
 \end{aligned}$$

We utilise the parameter setting  $\alpha_0 = 0.03, \alpha = 29.97, k_m = 40, n = 3, k_{\{lp, tp, cp\}} = 0.069, k_{\{lr, tr, cr\}} = 6.93, k_{\{lr2, tr2, cr2\}} = 0.347$  resulted from a parameter fitting based on the available experimental data (Garcia-Ojalvo et al., 2004). Additionally, the initial species concentrations in case of no phase shift are chosen at the limit cycle, e.g.  $lr = 0.819, tr = 2.388, cr = 0.068, lp = 36.263, tp = 166.685, cp = 64.26$ .

The repressilator's oscillation frequency mainly depends on the degradation reaction rates. Diffusion of TetR proteins from one repressilator to its adjacent counterpart causes the same effect. This allows to control the frequency just by forcing using a sustained dissipation of diffusing TetR proteins. Fig. 2 illustrates a typical synchronisation run.

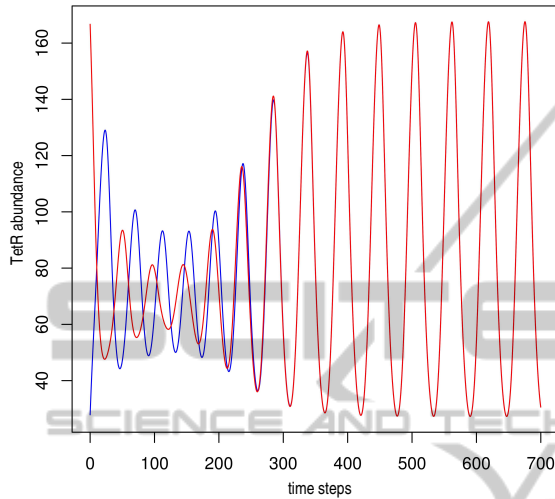


Figure 2: Typical synchronisation run of two coupled repressilators, coupling strength  $diff = 0.04$ , initial phase shift  $182^\circ$  (arbitrarily chosen). Simulation carried out with Co-pasi using ODEs and parameter settings given in Sec. 2.1.

## 2.2 Synchronising Initial Phase Shifts

For the synchronisation study, we set up both repressilator's initial concentrations at the individual limit cycle in order to avoid effects occurring within the transient phase (stabilisation phase). Afterwards, a two-dimensional parameter scan was conducted varying the initial phase shift of both repressilators between  $0^\circ$  and  $360^\circ$  and simultaneously varying the coupling strength within the relevant range  $diff = 0.01$  to  $0.13$  (weak to strong coupling). The time to synchronisation was obtained assuming a signal convergence of one minute per day ( $\epsilon$ -neighbourhood's interval length =  $\frac{1}{1440}$  of oscillation period), see Fig. 3.

The simulation study exhibits a correlation between coupling strength ( $diff$ ) and time to synchronisation. Since a strong coupling ( $diff = 0.13$ ) has a more significant effect on the adjacent repressilator's behaviour, synchronisation is achieved fast. In this case, even the influence of different initial phase shifts can be widely neglected. The situation becomes different when considering a weak coupling. Here, the initial phase shift predominantly determines the time to synchronisation. Initial antiphase rhythmicity (phase shift  $180^\circ$ ) between both repressilators causes

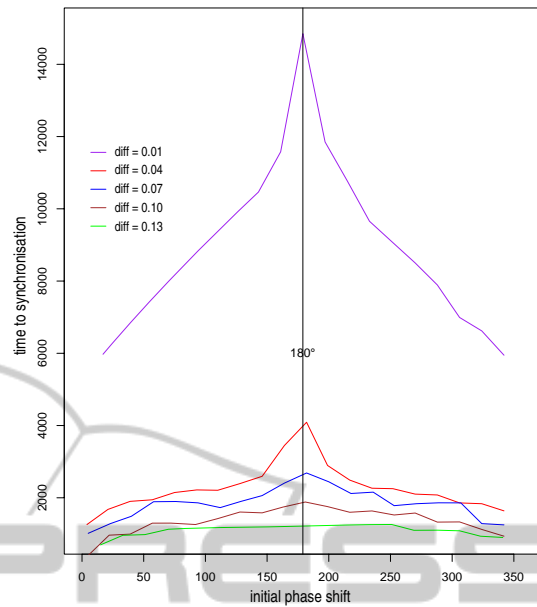


Figure 3: Time to synchronisation subject to various initial phase shifts. Parameter  $diff = 0.01, \dots, 0.13$  denotes coupling strength from weak to strong coupling. Initial antiphase rhythmicity (phase shift  $180^\circ$ ) between both repressilators causes the highest effort to synchronise both oscillatory signals by mutual forcing.

the highest effort to synchronise both oscillatory signals by mutual forcing. In this context, it is interesting to mention that the ability of the repressilator coupling to synchronise initial antiphase rhythmicity is a direct consequence of the (slight) asymmetric oscillatory signal shape. While symmetric oscillation curves (like sinusoidal signals) persist in antiphase when coupled, hence unable to synchronise, asymmetric curves (like spiking signals) entail a kind of unbalanced response to forcing. There is no equilibrium between forcing effects shortening and those advancing the oscillatory period. The remaining effect is sufficient to initiate synchronisation. The slight asymmetry of the diagram in Fig. 3 also results from the asymmetric shape of the repressilator's oscillatory signal. Interestingly, a medium coupling strength ( $diff = 0.07$ ) generates a behaviour in which time to synchronisation for increasing initial phase shift can be compensated within a range of approximately  $50^\circ \dots 100^\circ$  and  $260^\circ \dots 310^\circ$ , respectively.

## 2.3 Synchronisation of Different Initial Frequencies

We demonstrate the ability of the repressilator coupling to synchronise different initial frequencies in the elementary repressilators. To this end, individual pro-

tein degradation rates  $k_{lp}, k_{ip}, k_{cp}$  had been modified in conjunction with setting up all initial concentrations at the individual limit cycle. From this, we conducted a parameter scan taking into account the ratios of initial frequencies.

The purpose of this case study is to answer four questions: (1) Is there any synchronisation window, a continuous range of parameter settings, that runs the entire system into synchronisation? In other words, can we detect a variant of a so-called Arnold tongue? (2) If a synchronisation window could be identified, which of the three conditions necessary for synchronised oscillations become violated by leaving the delimiting parameter settings? (3) How is the time to synchronisation distributed within the synchronisation window? (4) Which synchronous frequency does result from the initially different frequencies after synchronisation?

While question (1) seems suitable to be answered in part using the Kuramoto method (Kuramoto, 1984), an analytical ODE-based technique, a sufficient clarification of questions (2), (3), and (4) requires an explorative simulation study. An essential part of this study is the calculation of the frequencies governed by an oscillatory signal. To this end, we utilise the discrete Fast Fourier Transformation (FFT) for long-term data accompanied by sampling and counting of local oscillatory signals maxima or minima for short-time data series. Time to synchronisation is again measured by the number of elapsed time steps up to convergence of one minute per day (cf. Sec. 2.2).

If synchronisation is obtained, we can distinguish two qualitative scenarios characterised by the resulting synchronous frequency in relation to either initial frequencies.

Fig. 4 depicts a typical temporal course towards synchronisation of two *marginally* different initial frequencies (solid lines). During the synchronisation process, both frequencies converge to a common value (dashed curves). This value deviates from both initial frequencies but arises in between. The synchronisation itself runs rather fast.

In contrast, a stronger – however *slight* – deviance of initial frequencies turns the synchronisation into a final frequency asymptotically converging to the maximum initial frequency, see Fig. 5 for an example. Here, the synchronisation process takes more time.

The latter case coincides with arrival at the limits of the synchronisation window marking the maximal deviance of initial frequencies leading to synchronisation. Inside the synchronisation window, the synchronous frequency becomes adjusted in between of both initial frequencies, and the more we approach towards the boundaries of the synchronisation window,

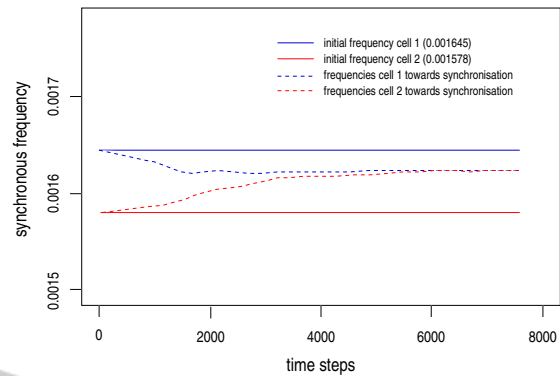


Figure 4: Typical temporal course towards synchronisation of two marginally different initial frequencies (solid lines) converging to a common value (dashed curves). Coupling strength:  $diff = 0.01$ , ratio of initial frequencies:  $\frac{0.001645}{0.001578} \approx 1.042$ . Synchronous frequency: 0.001616.

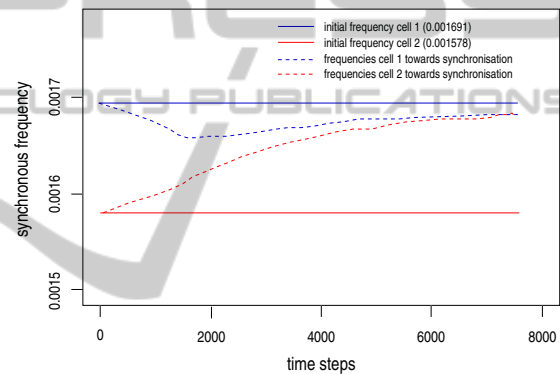


Figure 5: Typical temporal course towards synchronisation at the boundary of the synchronisation window. Synchronous frequency asymptotically reaches the maximum of either initial frequencies (dashed curves). Initial frequencies marked by solid lines. Coupling strength:  $diff = 0.01$ , ratio of initial frequencies:  $\frac{0.001691}{0.001578} \approx 1.072$ . Synchronous frequency: 0.001690.

the synchronous frequency converges to the maximum of both initial frequencies.

We obtain a synchronisation window delimited by polyfrequental oscillations with respect to the ratios of initial frequencies and loss of undamped oscillation with respect to the coupling strength, see Fig. 6. We checked whether an oscillatory signal is undamped or not by evaluating the eigenvalues of the Jacobian matrix derived from the ODEs specifying the reaction-diffusion kinetics.

Moreover, the simulation results indicate that a medium coupling strength ( $diff = 0.07$ ) enables synchronisation within the largest ratio of initial frequencies ranging from 0.697 to 1.294. This means in terms of systems application for clock synchronisation that a clock signal can be temporarily slowed down (post-

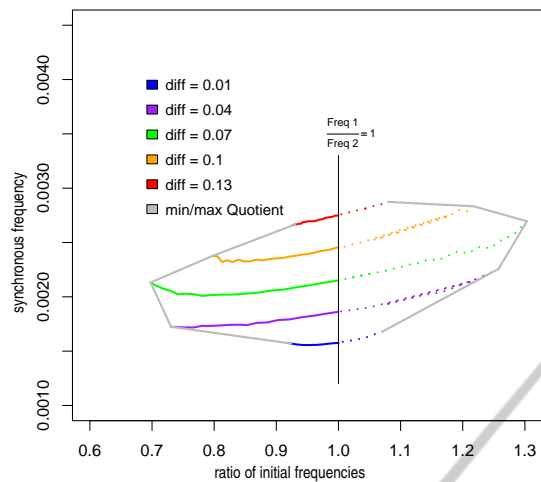


Figure 6: Synchronisation window: ratios of initial frequencies subject to synchronous frequency considering a variety of relevant coupling strengths  $diff = 0.01, \dots, 0.13$  (variant of an Arnold tongue, a circle map disclosing dependencies of system parameters within a range of stable oscillation). Due to the bidirectionally balanced coupling strength, an almost symmetric synchronisation window can be obtained which is delimited by polyfrequent oscillations with respect to the ratios of initial frequencies and loss of undamped oscillation with respect to coupling strength.

pone the clock) and speeded up (put the clock forward) with up to approximately 30% of its velocity. The knowledge about parameterisation, capabilities and limits of an oscillatory system envisioned to act as a biological clock is essential for subsequent integrative modelling, synthesis, and implementation of a corresponding frequency control system.

Bidirectionally coupled repressilators exhibit the ability to synchronise their oscillatory signals by forcing. It has been observed that arbitrary initial phase shifts become compensated while an adaption of the entire system to different initial frequencies of the single oscillators spans a synchronisation window.

### 3 EXTERNAL SYNCHRONISATION: REPRESSILATOR AS CORE OSCILLATOR

The repressilator can be seen as an advantageous tool to conduct external synchronisation when embedded as core oscillator into a frequency control system based on the concept of phase-locked loop (Stensby, 1997), PLL for short. These systems adapt their oscillatory output signal to an external stimulus acting as reference. In contrast to internal synchronisation, the

external stimulus is not affected. A biological example is given by circadian clocks that harmonise their oscillatory behaviour with the daily light-dark rhythmicity (Bell-Pedersen, 2005). Here, the light acts as external stimulus. Fig. 7 illustrates the general scheme of PLL. One or several coupled core oscillators constitute its central part. The signal comparator as downstream module determines the difference between core oscillator output and external stimulus. The phase shift between either signals is an ideal candidate to form an error signal able to adjust the core oscillator. The error signal passes a global feedback path along with damping and delay by dedicated low-pass filters. Finally, the resulting smoothed signal influences the core oscillator(s) by increasing or decreasing its frequency.

We expect to demonstrate that all functional modules required for a PLL control system can be implemented as interacting reaction networks. Both modules, signal comparator and global feedback path, efficiently employ low-pass filters. Signal transduction cascades found in cell signalling networks are a common biological motif to cover the functionality of low-pass filters (Marhl et al., 2005). Here, a focal protein alters its chemical state according to a trigger signal. Here, a chemical state is specified by addition or removal of phosphate groups to/from the focal protein. In case of low-frequency triggers, the subsequent modification of the chemical state can follow. Along with increasing frequency of the trigger, a threshold exists denoting that the reaction system is now too slow to follow the trigger and ends up in a steady state by means of a chemical equilibrium.

Having a chemical low-pass filter at hand, the functionality of the global feedback path is completely covered. The signal comparator benefits from low-pass filters to obtain the fundamental frequency of both signals, core oscillator output and external stimulus. Then, the phase shift between both signals or the signal difference, respectively, can be extracted by performing arithmetic operations. Reaction networks to this task are effectively feasible assuming that substrate species concentrations encode operands while product species concentrations (in steady state) constitute the operational output (Hinze et al., 2009). For example, the set of two reactions  $X_1 + X_2 \rightarrow Y$  and degradation  $Y \rightarrow \emptyset$  in conjunction with mass-action kinetics conducts a multiplication of the form  $Y = X_1(0) \cdot X_2(0)$  with initial concentrations  $X_1(0)$  and  $X_2(0)$  as multipliers. Addition, non-negative subtraction, and division can be expressed in a similar way. Altogether, this allows construction of a PLL explicitly composed of reaction-diffusion networks.

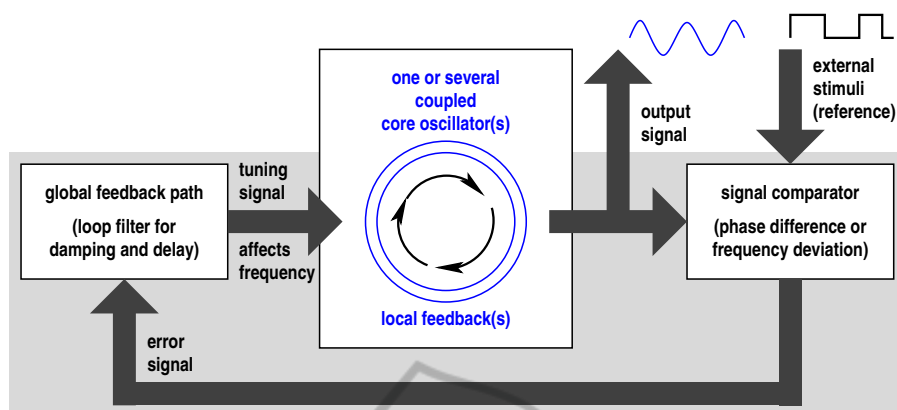


Figure 7: General scheme of a frequency control system based on the concept of phase-locked loop (PLL). The system adapts its oscillatory output signal to an external stimulus acting as reference for external synchronisation.

## 4 CONCLUSIONS

Bidirectionally coupled repressilators synchronise their oscillatory signals by forcing. Arbitrary initial phase shifts become compensated while adaptation to different initial frequencies spans a synchronisation window. Coupled repressilators can be seen as a part of a biological control system based on the concept of phase-locked loops. Further research has been directed to finalise the entire frequency control system by integration of additional components for signal comparison and damping, demonstrated by low-pass filters biologically implemented as specific signal transduction cascades. The simulations described in this paper were carried out using Copasi (Hoops, 2006), statistical evaluation using [R].

## ACKNOWLEDGEMENTS

We gratefully acknowledge funding from the German Federal Ministry of Education and Research (project no. 0315260A, Research Initiative in Systems Biology).

## REFERENCES

- Bell-Pedersen, D. (2005). Circadian rhythms from multiple oscillators: lessons from diverse organisms. *Nat. Rev. Genet.*, 6:544–556.
- Elowitz, M. B. and Leibler, S. (2000). A synthetic oscillatory network of transcriptional regulators. *Nature*, 403:335–338.
- García-Ojalvo, J., Elowitz, M., and Strogatz, S. (2004). Modeling a synthetic multicellular clock: repressila-

tors coupled by quorum sensing. *Proc. Natl. Acad. Sci. U.S.A.*, 101:10955–10960.

- Granada, A. and Herzog, H. (2009). How to achieve fast entrainment? the timescale to synchronization. *PLoS ONE* 4, e7057.
- Hinze, T., Fassler, R., Lenser, T., and Dittrich, P. (2009). Register machine computations on binary numbers by oscillating and catalytic chemical reactions modelled using mass-action kinetics. *International Journal of Foundations of Computer Science*, 20(3):411–426.
- Hoops, S. (2006). COPASI – a COMplex PATHway Simulator. *Bioinformatics*, 22:3067–3074.
- Kuramoto, Y. (1984). *Chemical oscillations, waves, and turbulences*. Springer.
- Marhl, M., Perc, M., and Schuster, S. (2005). Selective regulation of cellular processes via protein cascades acting as band-pass filters for time-limited oscillations. *FEBS Letters*, 579(25):5461–5465.
- Pikovsky, A., Rosenblum, M., and Kurths, J. (2001). *Synchronization: A universal concept in nonlinear sciences*. Cambridge University Press.
- Russo, G. and di Bernardo, M. (2009). How to synchronize biological clocks. *Journal of Computational Biology*, 16:379–393.
- Stensby, J. (1997). *Phase-locked loops*. CRC Press.
- Tanenbaum, A. S. and van Steen, M. (2001). *Distributed Systems: Principles and Paradigms*. Prentice Hall International.